Title

CRISPR-Mediated Genomic Addition to CPS1 Deficient iPSCs is Insufficient to Restore Nitrogen Homeostasis.

Journal

Yale Journal of Biology and Medicine, 94(4)

Authors

Nitzahn, Matthew
Truong, Brian
Khoja, Suhail
et al.

Publication Date

2021-12-01

Peer reviewed

YALE JOURNAL OF BIOLOGY AND MEDICINE 94 (2021), pp.545-557.

ORIGINAL CONTRIBUTION

YALE JOURNAL OF BIOLOGY AND MEDICINE
YJBM
CELEBRATING 90 YEARS 1928–2018

CRISPR-Mediated Genomic Addition to CPS1 Deficient iPSCs is Insufficient to Restore Nitrogen Homeostasis

Matthew Nitzahn[a,b], Brian Truong[b,c], Suhail Khoja[b], Agustin Vega-Crespo[c], Colleen Le[b], Adam Eliav[b], Georgios Makris[d], April D. Pyle[e,f], Johannes Häberle[d], and Gerald S. Lipshutz[a,b,c,g,h,i,*]

[a]Molecular Biology Institute, David Geffen School of Medicine at UCLA, Los Angeles, CA, USA; [b]Department of Surgery, David Geffen School of Medicine at UCLA, Los Angeles, CA, USA; [c]Department of Molecular and Medical Pharmacology, David Geffen School of Medicine at UCLA, Los Angeles, CA, USA; [d]Division of Metabolism and Children's Research Center, University Children's Hospital Zurich, Switzerland; [e]Department of Microbiology, Immunology, and Molecular Genetics, David Geffen School of Medicine at UCLA, Los Angeles, CA, USA; [f]Eli and Edythe Broad Stem Cell Center, David Geffen School of Medicine at UCLA, Los Angeles, CA, USA; [g]Department of Psychiatry, David Geffen School of Medicine at UCLA, Los Angeles, CA, USA; [h]Intellectual and Developmental Disabilities Research Center, David Geffen School of Medicine at UCLA, Los Angeles, CA, USA; [i]Semel Institute for Neuroscience, David Geffen School of Medicine at UCLA, Los Angeles, CA, USA

CPS1 deficiency is an inborn error of metabolism caused by loss-of-function mutations in the *CPS1* gene, catalyzing the initial reaction of the urea cycle. Deficiency typically leads to toxic levels of plasma ammonia, cerebral edema, coma, and death, with the only curative treatment being liver transplantation; due to limited donor availability and the invasiveness and complications of the procedure, however, alternative therapies are needed. Induced pluripotent stem cells offer an alternative cell source to partial or whole liver grafts that theoretically would not require immune suppression regimens and additionally are amenable to genetic modifications. Here, we genetically modified CPS1 deficient patient-derived stem cells to constitutively express human codon optimized CPS1 from the *AAVS1* safe harbor site. While edited stem cells efficiently differentiated to hepatocyte-like cells, they failed to metabolize ammonia more efficiently than their unedited counterparts. This unexpected result appears to have arisen in part due to transgene promoter methylation, and thus transcriptional silencing, in undifferentiated cells, impacting their capacity to restore the complete urea cycle function upon differentiation. As pluripotent stem cell strategies are being expanded widely for potential cell therapies, these results highlight the need for strict quality control and functional analysis to ensure the integrity of cell products.

*To whom all correspondence should be addressed: Gerald S. Lipshutz, David Geffen School of Medicine at UCLA, Los Angeles, CA 90095-7054; Email: glipshutz@mednet.ucla.edu.

Abbreviations: CPS1, carbamoyl phosphate synthetase 1; iPSC, induced pluripotent stem cell; hcoCPS1, human codon-optimized CPS1; CRISPR, clustered regularly interspaced short palindromic repeats.

Keywords: Carbamoyl phosphate synthetase deficiency, hyperammonemia, gene therapy, CRISPR/Cas9, iPSC

Author Contributions: MN and GSL: Experimental design, data acquisition, interpretation, analysis, manuscript preparation. BT, SK, AVC, CL, AE, GM, ADP, JH: Data acquisition, analysis, critical review of the manuscript.

INTRODUCTION

Carbamoyl phosphate synthetase 1 (CPS1, EC 6.3.4.16) deficiency (OMIM #237300) is a rare inborn error of metabolism affecting the first, rate-limiting enzyme of the urea cycle, the hepatocyte function in terrestrial mammals that incorporates waste ammonia into urea for excretion; this disorder affects 1 in 300,000 to 1 in 1.3 million live births worldwide [1,2]. Functional impairment or loss of CPS1 typically results in elevated plasma ammonia without orotic aciduria, leading to nausea, lethargy, encephalopathy, and coma [3]. These symptoms rapidly progress and may lead to death despite rapid diagnosis and aggressive treatments including hemodialysis and ammonia scavenger drugs [4-6]. However, even if these treatments are successful in mitigating acute plasma ammonia elevations, they are incapable of preventing recurrent crises and the irreversible neurocognitive damage associated with them.

As a monogenic disorder with well-defined biochemistry, CPS1 deficiency represents a seemingly prime target for classic gene therapy approaches. Recent gene therapy successes for all the other urea cycle enzymes [7-10] also encourage this approach, but CPS1 has multiple unique hurdles that make implementing such strategies difficult, including relatively high therapeutic threshold [11] and relatively large cDNA size. These challenges were recently overcome using helper-dependent adenovirus- [12] and dual adeno-associated virus (AAV)-based [13] gene replacement approaches, both demonstrating that lost murine Cps1 expression could be replaced with ectopic expression of murine or human CPS1, respectively. Though successful, the adenoviral approach is limited by potential immune complications [14]; in addition, the dual AAV strategy is at present somewhat limited by high viral loads that may be impractical for production and patient administration. Both viral strategies may be further impacted by waning efficacy over time due to episomal loss.

Cell-based therapies for metabolic disorders in general, and CPS1 deficiency in particular, may provide a viable alternative to virus-based gene therapies. Liver transplantation is generally curative but requires long-term immune suppression and faces continued scarcity in supply of donor organs [3]; in addition, patients often still require dietary supplementation of citrulline (a key urea cycle intermediate) [15]. Patient-derived induced pluripotent stem cells (iPSCs) could circumvent the issues associated with finding compatible donor organs as well as viral delivery of genetic materials. Successful cell replacement with exogenous hepatocytes has been reported in some studies for metabolic disorders [16-18], including CPS1 deficiency [19], though rigorous and well-controlled trials remain to be performed. Human hepatocyte transplantation in an immunosuppressed murine model has previously been shown to treat another urea cycle disorder, arginase 1 deficiency [20], effectively, and iPSC-derived hepatocytes are beginning to show similar promise in some enzyme activities when compared to primary hepatocytes [21]. An important advantage of iPSC-derived hepatocyte-like cells (HLCs) is that cell quality can be controlled prior to transplantation, potentially generating a functionally unlimited supply of hepatocytes to replace the endogenous dysfunctional cells.

The discovery and implementation of the clustered regularly interspaced short palindromic repeats (CRISPR)/Cas9 gene editing platform [22,23] has revolutionized genome editing in recent years, providing a rapid and reliable tool to make precise modifications. Multiple types of mammalian cells have been edited with CRISPR/Cas9, including human iPSCs [24]. One advantage of using patient-derived iPSCs for *in vitro* editing, as opposed to primary cells *ex vivo*, is that targeted changes can be rigorously validated by sequencing prior to transplantation; in addition, potential off-target cleavage events can be predicted and mitigated through careful design, and also subsequently confirmed. iPSCs edited with CRISPR/Cas9 have been shown to robustly express transgenes [25], including those of urea cycle enzymes [26], making this an attractive option for CPS1 deficiency.

Herein, we reprogrammed patient-derived CPS1 deficient fibroblasts to iPSCs and subsequently utilized CRISPR/Cas9 to introduce ectopic CPS1 expression from the AAVS1 safe harbor locus in a genomic addition approach. The resultant cells were then differentiated to HLCs to assess their ammonia metabolizing capability.

RESULTS

Reprogramming of CPS1 Deficient Fibroblasts Successfully Produces Pluripotent Stem Cells

To establish a human cell model for CPS1 deficiency, we acquired three deidentified patient fibroblast lines, termed CD1, CD2, and GM03432 (the latter subsequently referred to as GM) (Figure 1A). Clinical reports from all three patients indicated each had neonatal onset of disease symptoms; CD1 cells are from an afflicted male, while CD2 and GM cells are from afflicted females. CD1 cells contain a homozygous nonsense mutation resulting from the transversion c.2494G>T, leading to amino acid residue 832 converting from glutamate to a stop codon (E832X). CD2 is compound heterozygous with c.2740G>C, changing aspartate 914 to histidine (D914H), and a splice mutation resulting in exon 36 skipping (c.4162-2A>G). GM also contains a homozygous mutation, but it is missense c.610G>T, resulting in a valine to phenylalanine transition at residue 204 (V204F).

A

Line Name	Sex	Disease Onset	Mutation
CD1	Male	Neonatal	E832X
CD2	Female	Neonatal	D914H c.4162-2A>G
GM	Female	Neonatal	V204F

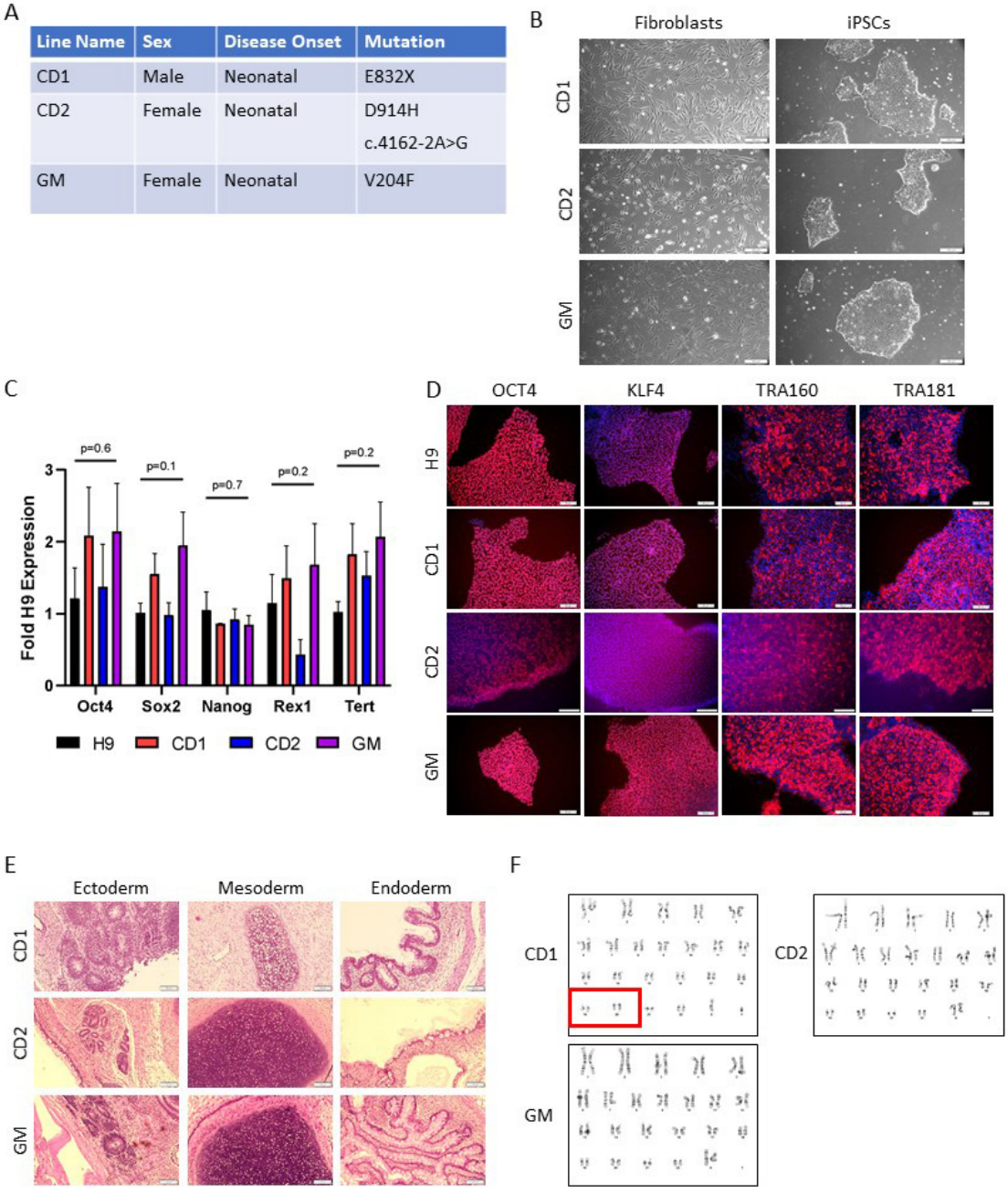

Figure 1. **Characterization of patient-derived iPSCs**. **A**. Table detailing the mutations in the three cell lines. CD1 and GM are both homozygous, while CD2 is compound heterozygous. **B**. Bright field images of patient-derived parental fibroblasts and their corresponding daughter iPSCs. **C**. Fold change qPCR analysis of pluripotency genes in patient iPSCs compared to the human embryonic stem cell line H9 (normalized to 1). Data are mean ± SEM, n = 3 per group. P values are from one-way ANOVA. **D**. Immunocytochemistry of pluripotency markers in iPSCs compared to H9 cells. **E**. H&E staining of sections from teratomas formed by each cell line. All three lines generate tissues derived from the three primary germ layers. **F**. Karyotype analysis of CD1 (top left panel), CD2 (top right panel), and GM (bottom left panel) iPSCs. Red box in CD1 indicates balanced chromosomal translocation between chromosomes 19 and 20.

These three lines were reprogrammed using a lentivirus expressing the four classic Yamanaka factors OCT4, SOX2, KLF4, and MYC, and clones from each cell line were used for characterization. All iPSCs exhibited typical morphology (Figure 1B), and gene expression analysis demonstrated that they express the pluripotency genes *OCT4*, *SOX2*, *NANOG*, *REX1*, and *TERT* at similar levels to the established human embryonic stem cell line H9 (Figure 1C), chosen as a well-characterized reference of pluripotency. Immunocytochemistry showed that these cells express the pluripotency markers OCT4, KLF4, TRA-160, and TRA-181 at the protein level (Figure 1D). When injected into immunocompromised mice, cells were also capable of forming teratomas with tissue derived from all three germ layers (Figure 1E). Karyotype analysis demonstrated that CD2 and GM iPSCs have no detectable large chromosomal aberrations (Figure 1F); however, CD1 was found to have a balanced translocation between the short arm of chromosome 19 and the long arm of chromosome 20 (red box). This mutation was also identified in the parental fibroblasts, however; thus, this was not a result of reprogramming. A single clone from each line was chosen for all downstream experiments.

CRISPR/Cas9-Mediated Genomic Addition Successfully Inserts Human Codon Optimized CPS1 into the AAVS1 Safe Harbor Locus

To restore expression in CPS1 deficient cell lines, human codon-optimized CPS1 cDNA (hcoCPS1) was introduced into the *AAVS1* safe harbor locus using two guide RNAs and Cas9 nickase as in the previously described AFP reporter cell (ARC) vector [27] with modifications. Here, the human *EF1α* promoter drives the expression of hcoCPS1, which is terminated by the human growth hormone polyadenylation sequence. An in-frame puromycin resistance gene allows for drug selection of transfected cells after integration, with the entire cassette flanked by homology arms to *AAVS1*. A schematic of the genome editing strategy is depicted in Figure 2A.

After integration, puromycin-resistant cells were subcloned, and genomic DNA was extracted to determine if integration had been faithfully completed. PCR analysis of both the 5' and 3' junctions was performed using primer pairs amplifying from outside of the homology arms and inside the transgenic cassette (Figure 2A, black and blue arrows); the expected bands were present in edited cells but not in unedited cells (Figure 2B). Junction PCR products were subsequently sequenced, demonstrating seamless integration of the expected genomic region and transgene sequences without errors (Figure 2C).

Differentiation of iPSCs Resulted in Hepatocyte-Like Cells Inefficient in Ammonia Metabolism

To determine the capacity of these iPSCs to form hepatocyte-like cells (HLCs), iPSCs were differentiated using a previously described method [28]. Figure 3A depicts the overall differentiation strategy. After a 4-day endoderm induction, cells were incubated for 8 days with hepatocyte growth factor (HGF) and dimethylsulfoxide (DMSO) to induce hepatic specification, followed by 6 days in dexamethasone, an extension of 3 days from the original protocol that modestly improves urea cycle gene expression [27]. The subsequently produced HLCs were maintained for 3 days in the presence of dexamethasone, hydrocortisone, insulin, and DMSO before being harvested for analysis on day 21. Day 21 HLCs from all three lines, both unedited and edited, exhibited the characteristic hepatocyte cobblestone morphology (Figure 3B). Edited cells did not statistically significantly differ from unedited cells in maturity based on expression of the immature hepatocyte gene α-fetoprotein (AFP; $p = 0.5$) and mature genes cytochrome p450 3A4 (CYP3A4; $p = 0.3$) and fumarylacetoacetate hydrolase (FAH; $p = 0.8$) (Figure 3C); additionally, edited and unedited cells both secreted albumin at comparable levels (1095ng/day/million cells ± 507 vs. 595ng/day/million cells ± 377 [unedited vs. edited, respectively]; $p = 0.4$) (Figure 3D). To measure the ammonia consumption capacity of differentiated HLCs, NH_4Cl was added to cell media at a final concentration of 2.5mM; supernatants were harvested after 24 hours and assayed to measure ammonia levels. Unexpectedly, unedited cell supernatants contained significantly less ammonia than their edited counterparts as a whole (unedited: 539.1μM ± 32.0; edited: 1215.0μM ± 64.3; $p < 0.0001$) and within each individual cell line (CD1: 539.3μM ± 9.05 vs. 1302μM ± 56.8, $p < 0.001$; CD2: 612.6μM ± 81.1 vs. 990.5μM ± 89.8, $p < 0.05$; GM: 465.3μM ± 14.6 vs. 1351μM ± 8.4, $p < 0.0001$) ($n = 3$ for each cell line, total of $n = 9$ per group [unedited or edited]) (Figure 3E). Urea levels were below the limits of detection (data not shown).

Investigating Potential Mechanisms of Differential Ammonia Metabolism

To address the unexpected results from the *in vitro* ammonia challenge, RNA was extracted from HLCs and subjected to qPCR analysis for the 6 enzymes and 2 transporters of the urea cycle, in addition to hcoCPS1, to further assess function (Figure 4A). There were no significant differences in gene expression between unedited and edited HLCs ($n = 3$ per cell line, total $n = 9$ per group) except for endogenous *CPS1* (0.52-fold ± 0.15 decrease in edited cells; $p = 0.017$). Unexpectedly, hcoCPS1 expression was not markedly elevated in edited cells (1.82-fold ± 0.4; $p = 0.22$), prompting an investigation into the cause of this poor expression. Loss of hcoCPS1 expression was not due to heterochromatin formation as these cells re-

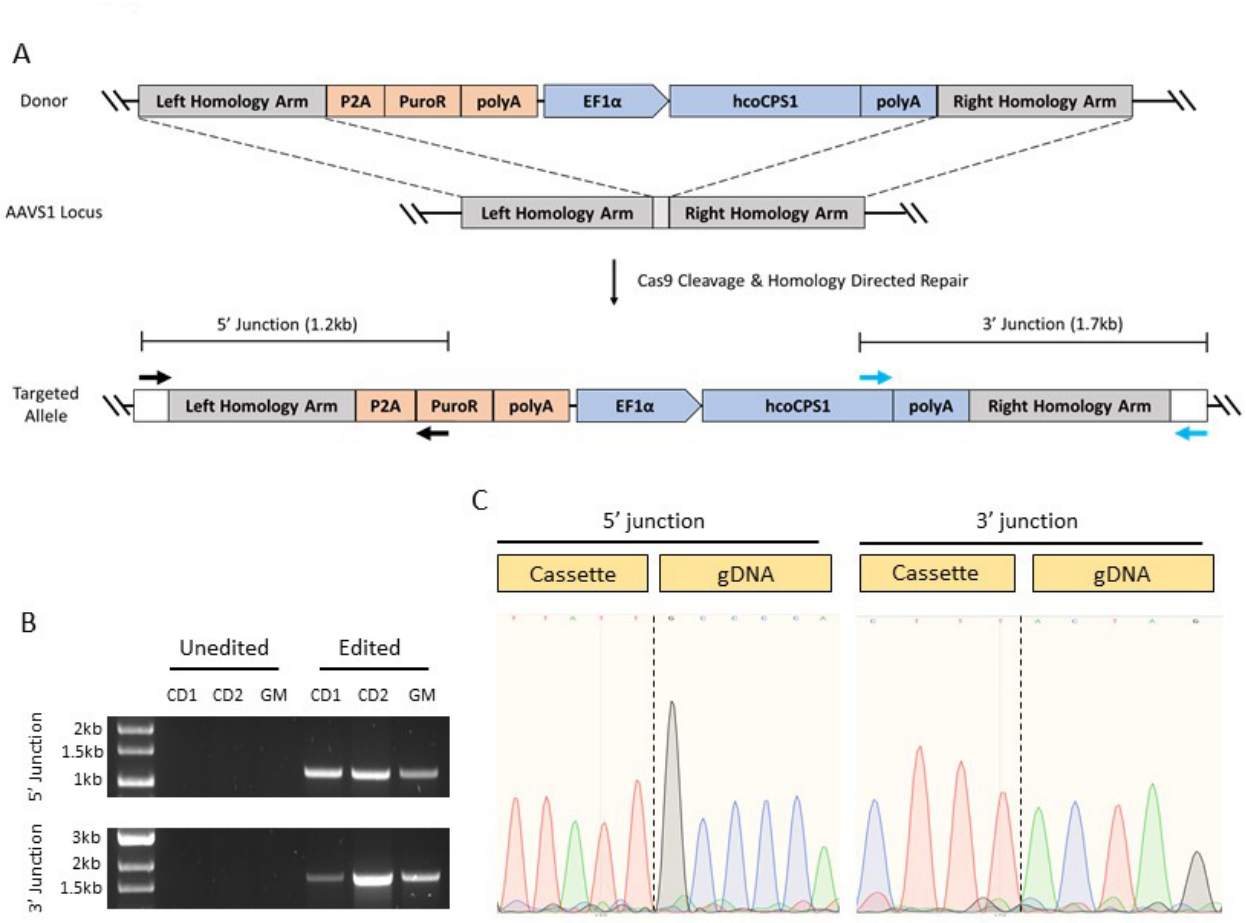

Figure 2. **Design and validation of CRISPR/Cas9 editing in iPSCs at the *AAVS1* locus**. **A**. Schematic of the overall CRISPR/Cas9 strategy. **B**. Gel images of PCRs amplifying either the 5' or 3' junctions, defined by the bracketed lines in (A). Primer locations are indicated by black arrows (5' junction) and blue arrows (3' junction) in (A). **C**. Sequencing of the 5' and 3' junctions showing faithful insertion of the transgenic construct.

tained puromycin resistance (data not shown), suggesting some other mechanism. DNA methylation is one method of gene regulation; cytosine residues in CpG dinucleotides are covalently methylated at the fifth position of the pyrimidine ring to form 5-methylcytosine. This event is commonly associated with transcriptional silencing [29]; global DNA methylation status is known to fluctuate during differentiation [30]. To determine the DNA methylation status at the transgene promoter in HLCs, genomic DNA was extracted and subjected to bisulfite conversion. Bisulfite conversion deaminates cytosine into uracil but has no effect on 5-methylcytosine. Subsequent sequencing can demonstrate if cytosines were protected from conversion by a methyl group, providing insight into local DNA methylation states. All three edited lines demonstrated methylation at all 19 CpG dinucleotides in the transgenic *EF1α* promoter, in addition to 7 CpGs in the flanking DNA (2 of them upstream and the remaining 5 downstream of the promoter) (Figure 4B). Unexpectedly, promoter methylation was not a result of differentiation as undifferentiated iPSCs also showed complete methylation at all CpGs (Figure 4C). The donor plasmid used during nucleofection showed no methylation (Figure 4C), indicating that promoter methylation was iPSC-derived after integration. Loss of hcoCPS1 expression was confirmed in iPSCs; shortly after CRISPR/Cas9 editing and puromycin selection, iPSCs showed significantly increased expression of hcoCPS1 (26.02-fold ± 11.16 compared to unedited; $p = 0.040$) (Figure 4D) which was lost upon subsequent culturing (1.76-fold ± 0.68 compared to unedited; $p = 0.7$) (Figure 4E). Transcriptional silencing was accompanied by undetectable levels of CPS1 enzyme activity in edited iPSCs (data not shown).

While promoter methylation explains the loss of hcoCPS1 expression, it fails to account for the difference in ammonia reduction (Figure 3D) between unedited and edited HLCs. Hepatocytes *in vivo* are central in regulating amino acid metabolism [31], including those whose

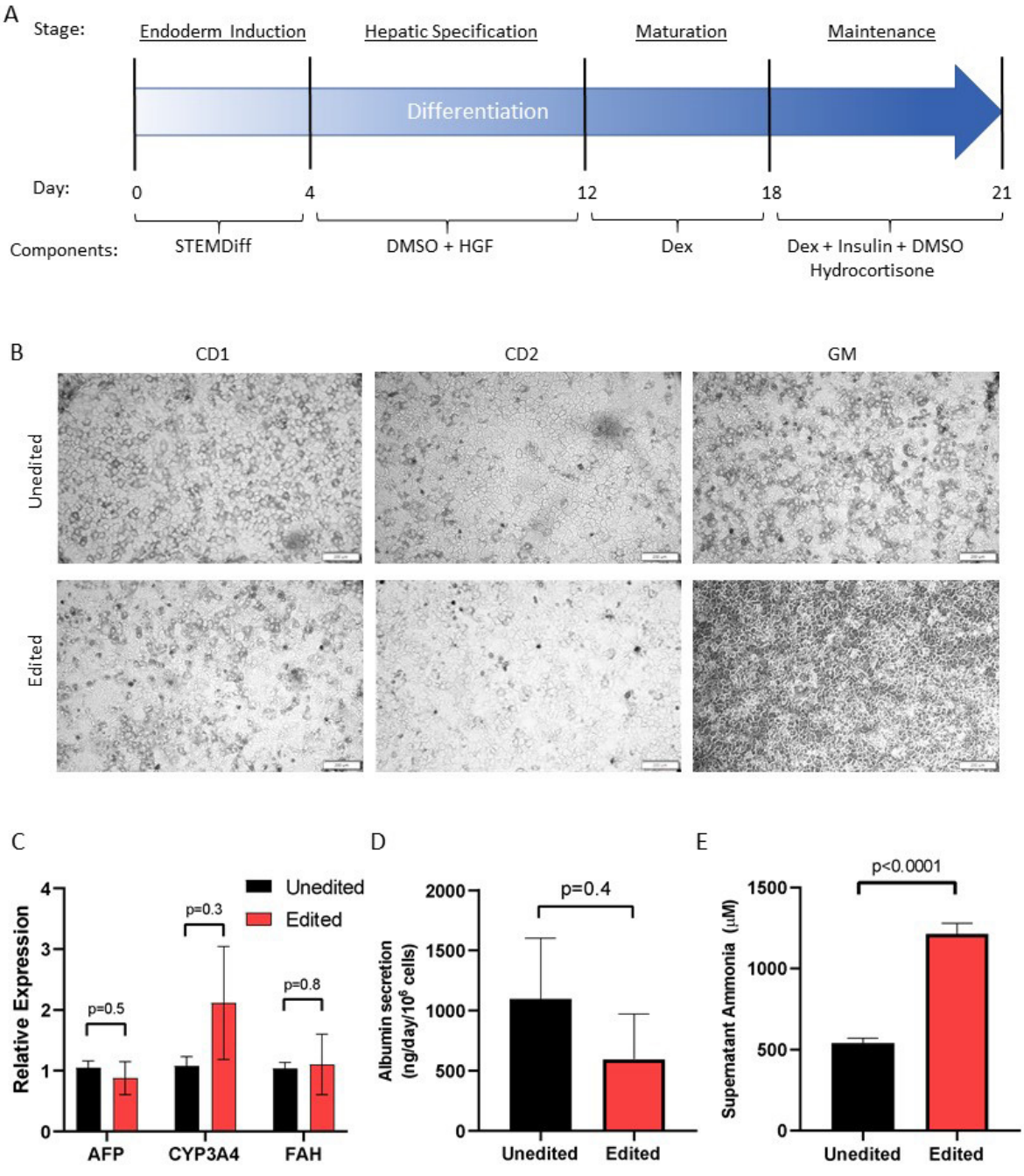

Figure 3. **Differentiation of iPSCs to HLCs**. **A**. Schematic diagram of the hepatic differentiation strategy. iPSCs are directed progressively through the definitive endoderm, hepatic specification, and maturation stages, using the listed growth factors to reach the HLC state. **B**. Representative bright field images of day 21 HLCs from all three lines with and without CRISPR/Cas9 genome editing. No salient morphological differences were observed. **C**. Fold change qPCR analysis of unedited (normalized to 1) and edited day 21 HLCs. Expression of the less mature *AFP* and more mature *CYP3A4* and *FAH* genes are not significantly different between the two. **D**. Levels of albumin secreted into cell culture media of day 21 HLCs after 24 hours. **E**. Levels of ammonia found in the supernatant of day 21 HLCs after 24 hours of treatment with 2.5mM NH_4Cl. Data in C-Eare mean ± SEM, n = 9 per group; n = 5 in edited group of (D).

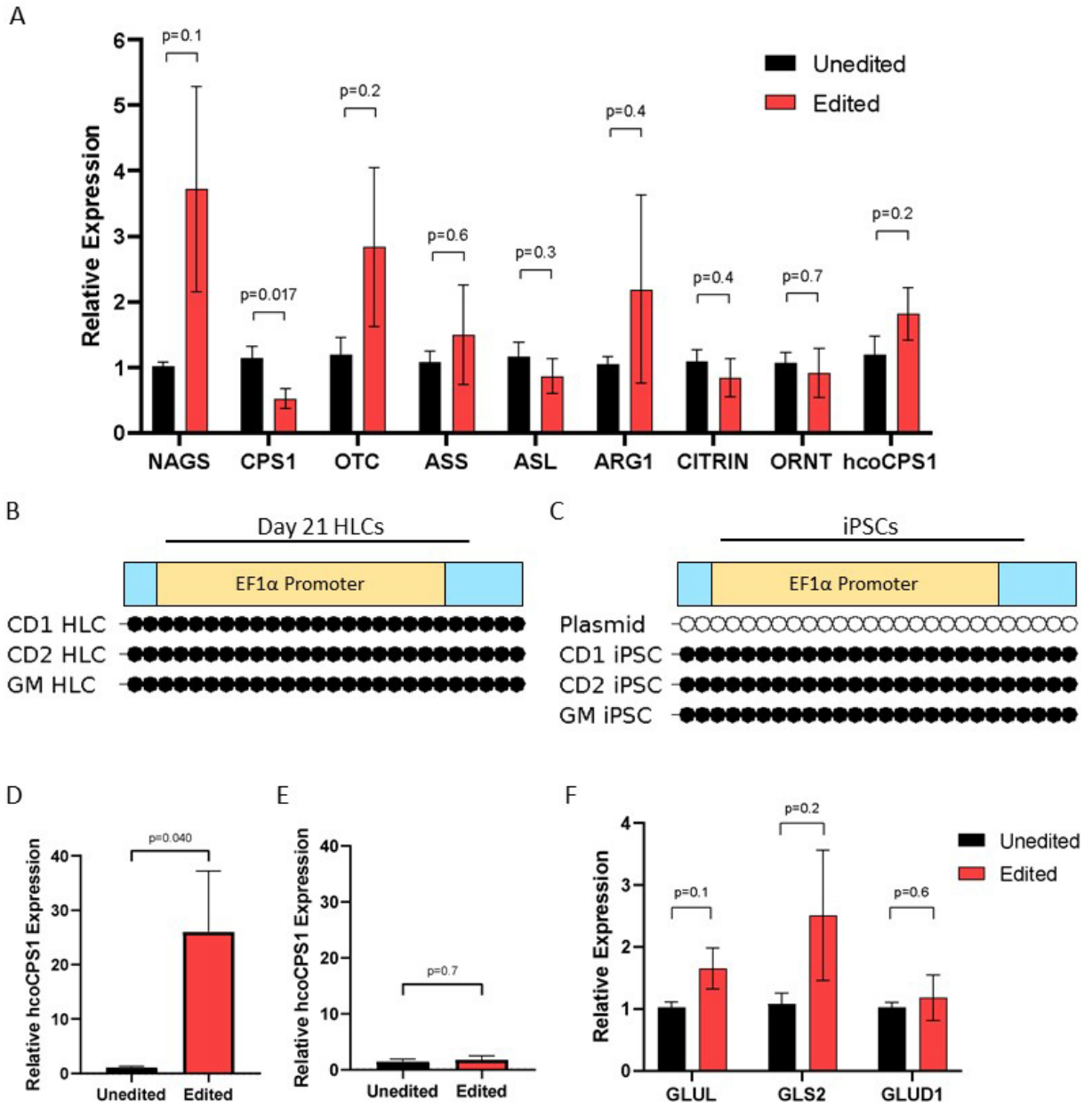

Figure 4. **Investigating the factors contributing to differential ammonia metabolism in unedited and edited HLCs**. **A**. Fold change qPCR of urea cycle-related genes (6 enzymes and 2 transporters) in day 21 HLCs, where unedited cell samples are normalized to 1. **B and C**. DNA methylation analysis of edited day 21 HLCs (B) and edited iPSCs with donor plasmid control (C). Unfilled circles represent unmethylated CpGs, while filled circles represent methylated CpGs. **D and E**. Fold change qPCR analysis of hcoCPS1 in unedited (normalized to 1) compared to edited iPSCs after only a few passages (D) and several passages (E). **F**. Fold change qPCR analysis of glutamate/glutamine metabolic genes in day 21 HLCs, where unedited cell samples are normalized to 1. Data in (A), (D), (E), and (F) are mean ± SEM, n = 9 per group.

synthesis involves the direct incorporation of ammonia. The reversible production of glutamine involves the condensation of glutamate with ammonia, regulated by glutamine synthetase (GLUL) and glutaminase 2 (GLS2). In addition, glutamate itself is reversibly produced from ammonia and α-ketoglutarate via the action of glutamate dehydrogenase (GLUD1). Because hcoCPS1 expression is lost in edited cells, we hypothesized that differential expression of any of these three metabolic genes could account for varying levels of ammonia utilization. However, qPCR analysis showed that none of these three genes were significantly differentially expressed between unedited and edited HLCs (*GLUL* p = 0.1; *GLS2* p = 0.2; *GLUD1* p = 0.6) (Figure 4F).

DISCUSSION

CPS1 deficiency is an inborn error of metabolism in which ureagenesis stalls due to lack of input carbamoyl phosphate from CPS1 enzymatic activity; waste nitrogen does not flux through the cycle thus preventing its eventual conversion to non-toxic urea that is excreted in urine. Symptoms typically arise in the neonatal period, though onset may occur at any time in childhood or into adulthood depending on the extent of protein dysfunction, with as many as 50% of neonatal cases leading to mortality [1]. Dietary protein restriction and ammonia scavenger drug administration are the mainstays of current therapy, but they are incompletely effective and have remained largely unchanged since the 1980s; orthotopic liver transplantation is generally curative, though donor organs remain scarce and the procedure is accompanied by lifelong immune suppression and its associated complications and risks; in some cases patients still require additional citrulline supplementation as small intestinal enterocytes remain CPS1 deficient [15]. Currently, there are no treatments that fully address the underlying biochemical imbalance or reverse the accumulated neurocognitive deficits from repeated episodes of hyperammonemia.

To develop a novel therapeutic option for CPS1 deficiency patients, we reprogrammed patient-derived fibroblasts into iPSCs and inserted human codon optimized CPS1 cDNA into the *AAVS1* locus for constitutive expression via the *EF1α* promoter using CRISPR/Cas9. Edited iPSCs were differentiated to HLCs to determine their ammonia metabolizing capacity relative to their isogenic, unedited controls. Upon challenging with NH_4Cl, edited HLCs removed significantly less ammonia from the supernatant than unedited HLCs. This was an unexpected outcome as overexpression of hcoCPS1, in the presence of similar expression levels of the other urea cycle enzymes, would be expected to increase ammonia utilization. However, upon further investigation, hcoCPS1 expression was found to be silenced due to promoter methylation.

The concept of using a safe harbor for genomic addition is not new; *AAVS1*-based transgene insertion and expression is a long-standing concept in stem cell biology and has many reported successes [32,33]. However, transgene silencing mediated by promoter methylation has also been reported in undifferentiated [34] and differentiated [32] cells. The present and prior studies suggest that promoter choice is a critical component in avoiding silencing. Previous work from our group [26] and others [35] has demonstrated that the *EF1α* promoter expresses well in PSCs, suggesting some other factor remains to be elucidated and is impacting methylation status. Cell-line specific alterations, and potentially global DNA methylation changes, may also exist that could explain the difference in unedited and edited cells. Therefore, preventing DNA methylation-dependent silencing, regardless of promoter choice, will need to be optimized prior to advancing iPSC-derived HLCs as a putative treatment option. This could be achieved using universal chromatin opening elements [36] or small molecule inhibitors of DNA methyltransferases [37], some of which are already FDA approved. Determining the causal factors of promoter silencing, and establishing innovations that resolve them, will be important in moving transgenic PSC technologies towards more translatable therapies.

The difference in ammonia utilization in unedited and edited HLCs, despite no obvious urea cycle-related gene expression differences (except for endogenous CPS1, the primers for which may have inefficient but non-negligible binding to hcoCPS1), suggests that unedited HLCs shuttled ammonia into an alternative pathway. In support of this notion, no difference was observed in urea formation between the two populations (data not shown) in preliminary experiments when treated with heavy isotope-labeled $^{15}NH_4$. In addition to urea, ammonia may be condensed with α-ketoglutarate to form glutamate by the enzyme glutamate dehydrogenase (GLUD1, EC 1.4.1.3). Glutamate may then receive an additional ammonia moiety to form glutamine via glutamine synthetase (GLUL, EC 6.3.1.2). Both reactions are reversible either by GLUD1 itself or by the action of glutaminase 2 (GLS2, EC 3.5.1.2), respectively. Together, these three enzymes represent a small portion of urea cycle-independent enzymes that directly or indirectly affect ammonia levels in hepatocytes, making them attractive targets to investigate as potential differential regulators of ammonia levels in unedited and edited HLCs. However, gene expression levels were not significantly different between the two cell populations, suggesting that if they are playing a role, then this is likely at the post-transcriptional level. Metabolic flux through these enzymes can be investigated using metabolomics approaches with $^{15}NH_4$ or

other isotopic nitrogen-containing compounds [38]; this may also clarify the roles of other processes affecting ammonia indirectly, such as amino acid uptake, in an unbiased way.

While there is great potential for iPSC-derived HLCs as a therapeutic, they do have important disadvantages. One significant drawback of utilizing iPSC-based technology for cell replacement is the time needed to generate, edit, and differentiate iPSCs to the desired fate. In metabolic disorders such as CPS1 deficiency, diagnosis can be made prenatally by amniocentesis [39] or chorionic villi biopsy [40], taking advantage of a key time window during which the unborn fetus relies on maternal ammonia clearance. This approach would potentiate the development of a cell-based therapeutic tailored to the patient that is ready for administration at or soon after birth. Recent advances in liver organoids [41] and scaffolding for transplantation [42] bring the potential of near-to-medium-future hepatocyte replacement therapies into sharper focus. As CPS1 deficiency has been treated in limited cases with primary hepatocyte transplantation [19], this approach has untapped therapeutic potential, especially in the context of ongoing donor liver scarcities [43].

In conclusion, these studies have demonstrated that CPS1 patient-derived iPSCs may be developed successfully to generate hepatocyte-like cells; however, *EF1α* promoter-driven hcoCPS1 expression from the *AAVS1* safe harbor is not suitable to reconstitute the urea cycle. This work lays a foundation for future studies investigating alternative promoter constructs and *cis*-regulatory elements to optimize transgene expression in differentiated cells and restore activity for this critical hepatic enzyme.

MATERIALS AND METHODS

Cell Lines and Reprogramming

Deidentified CPS1 deficiency patient fibroblasts were purchased from Coriell Institute for Medical Research (GM03432, Camden, NJ) or were a generous gift from Johannes Häberle (CD1 and CD2). The mutations in all lines were confirmed by Sanger sequencing (Laragen, Culver City, CA) and independently verified by exome sequencing performed by Prevention Genetics (Marshfield, WI). Fibroblasts were cultured on 0.1% gelatin (07903, StemCell Technologies, Vancouver, Canada) in DMEM/F12 (11320033) supplemented with 20% fetal bovine serum (FBS; 10437028), 1% glutaMAX (35050061), 1% non-essential amino acids (NEAA; 11140050, all from Invitrogen, Carlsbad, CA), and primocin (ant-pm-1, Invivogen, San Diego, CA). Fibroblasts were reprogrammed using the lentiviral STEMCCA vector expressing the four Yamanaka factors as described previously [26] and were subsequently cultured on irradiated mouse embryonic fibroblasts (A34180, ThermoFisher, Waltham, MA) in mTeSR Plus growth media (100-0276, StemCell Technologies) until colonies emerged. Clones were picked and transduced with AAV8-Cre (a gift from James M. Wilson, Addgene viral prep 105537-AAV8) to remove the STEMCCA cassette. Genomic DNA was harvested (69504, Qiagen, Hilden, Germany), and STEMCCA removal was confirmed by PCR as described (Center for Regenerative Medicine [CReM] iPSC Core of Boston University and Boston Medical Center https://www.bu.edu/dbin/stemcells/index_iPSC.php). Primers for STEMCCA PCR were: Forward: 5'-TGGCTCTCCTCAAGCGTATT-3'; Reverse: 5'-GTTGTGCATCTTGGGGTTCT-3'. iPSCs were routinely maintained on hESC-qualified Matrigel (354277, Corning Inc., Corning, NY) in mTeSR Plus and passaged using ReLeSR (05872, StemCell Technologies) according to the manufacturer's instructions.

Immunocytochemistry

iPSCs were probed for pluripotency markers as described previously [26]. Primary antibodies used were: OCT3/4 (SC-5279, Santa Cruz Biotechnology, Dallas, TX); KLF4 (RC-09-0021, Stemgent, Cambridge, MA); TRA1-60 (mab4360, MilliporeSigma, Burlington, MA); TRA1-81 (mab4381, MilliporeSigma) all at 1:200 dilutions. Secondary antibody used was goat anti-mouse IgG Alexa Fluor 488 (A-11001, Life Technologies, Carlsbad, CA) at 1:200 dilution.

qPCR

qPCR was performed as previously described [13]. Briefly, total RNA was isolated, and cDNA synthesized according to manufacturer's instructions (11828665001 and 4897030001, respectively, Roche, Basel, Switzerland). qPCR was carried out using ssoAdvanced Universal SYBRGreen (1725271, BioRad, Hercules, CA). A list of primers used can be found in Supplemental Table 1 (Appendix A). *GAPDH* was used as the housekeeping gene, and fold changes were calculated using the -ΔΔCt method.

Teratoma Assay

All mice were kept according to the National Institutes of Health guidelines and all experimental procedures were approved by and conducted according to the guidelines of the Institutional Animal Care and Use Committee of the University of California, Los Angeles. Mice had *ad lib* access to standard chow and water and were maintained on a 12-hour light-dark cycle. Severe combined immunodeficient mice (NOD.Cg-*Prkdc*^{scid} *Il2rg*^{tm1Wjl}/SzJ [NSG], Stock Number 005557, Jackson Laboratory, Bar Harbor, ME) were anaesthetized with isoflurane, and 10 million iPSCs suspended in Matrigel were injected unilaterally into the quadriceps. Mice were euthanized when

visible tumors formed, and the tissue was fixed in 10% buffered formalin for 48 hours. Teratomas were embedded in paraffin, sectioned, and stained with hematoxylin and eosin for imaging.

Hepatic Differentiation

iPSCs were differentiated to hepatocyte-like cells as described previously [28] with modifications. Undifferentiated iPSCs were incubated in 10μM Y-27632 ROCK inhibitor (SM-008, BioPioneer, San Diego, CA) for 1 hour and subsequently dissociated using Accutase (A1110501, ThermoFisher). Cells were then seeded onto Matrigel (CB-40230C, Corning Inc.) at a density of 2 million per well of a 6-well plate (approximately $2.1x10^5$ cells/cm^2). The following day, cells were induced to form endoderm using the STEMDiff Definitive Endoderm kit (5110, StemCell Technologies) for 4 days. Endodermal cells were then replated at ~50% density (empirically optimized for each individual cell line) in differentiation media made with DMEM/F12 containing 10% knockout serum replacement (10828028, Invitrogen), 1% NEAA, 1% glutaMAX, and primocin. This was further supplemented with 1% DMSO (D8418-500ML, MilliporeSigma) and 100ng/mL hepatocyte growth factor (78019, StemCell Technologies) for 8 days. Cells were then cultured for 6 days in differentiation media supplemented with 0.1μM dexamethasone (D4902-25MG, MilliporeSigma). Finally, cells were matured for 3 days in William's E media (12551032, Invitrogen) containing 10% FBS, 1% NEAA, 1% glutaMAX, 1.8% DMSO, 1μg/mL human insulin (I9278-5ML, MilliporeSigma), 4.8μg/mL hydrocortisone 21-hemisuccinate (H2270-100MG, MilliporeSigma), and 0.1μM dexamethasone. Media was changed daily throughout the differentiation. Cells were harvested using 0.25% trypsin (25200056, Invitrogen).

Molecular Cloning and CRISPR/Cas9 Genome Editing

Human codon-optimized *CPS1* (hcoCPS1) was synthesized by Blue Heron Biotech (Bothell, WA) as previously described [13]. hcoCPS1 was cloned into the ARC vector and inserted into the *AAVS1* site as described previously [27]. The plasmid ARC containing homology arms to *AAVS1*, a splice acceptor site, T2A, and puromycin resistance gene was used as the starting backbone, which was digested with KpnI and EcoRV to generate the vector backbone. NEBuilder HiFI DNA Assembly (E2621S, New England Biolabs, Ipswitch, MA) was used to introduce *EF1α*-driven hcoCPS1, along with the human growth hormone polyadenylation signal, into digested ARC, which was subsequently confirmed by sequencing, replacing the original transgenic construct and forming the new donor. This donor was nucleofected into iPSCs along with paired Cas9 nickases (a gift from Feng Zhang [44], Addgene #48140) targeting *AAVS1*, using the Amaxa Nucleofector (Lonza, Basel, Switzerland) program B016. Treated cells were then selected with puromycin at 1ug/mL. Clones were isolated and screened by PCR using the primers in Supplemental Table 1 (Appendix A). Faithful transgene integration was confirmed by sequencing (Laragen).

In Vitro Ammonia Challenge

Day 20 HLCs were treated with 2.5mM $^{15}NH_4Cl$ (Cambridge Isotope Laboratories, NLM-467-1), and supernatant was harvested after 24h and stored at -80°C until analysis as described previously [45-47]. Ammonia levels were detected using a colorimetric ammonia assay (ab83360, Abcam, Cambridge, UK) according to the manufacturer's instructions.

Albumin Secretion

Day 20 HLCs received fresh growth media, which was then harvested from day 21 HLCs after 24 hours. Albumin concentration was measured by ELISA according to the manufacturer's instructions (E80-129, Bethyl Laboratories, Montgomery, TX).

Urea Secretion

Day 20 HLCs received fresh growth media, which was then harvested from day 21 HLCs after 24 hours. Urea concentration was measured by colorimetric assay according to the manufacturer's instructions (EIBUN, ThermoFisher).

DNA Methylation Analysis

Genomic DNA from iPSCs and HLCs was isolated (69506, Qiagen) and subsequently bisulfite converted (D5005, Zymo Research, Irvine, CA) according to the manufacturer's instructions. The bisulfite-converted 231bp core *EF1α* promoter was PCR amplified and sequenced. Primers were designed using the Zymo Bisulfite Primer Seeker tool and are listed in Supplemental Table 1 (Appendix A).

Statistical Analysis

Collected data was analyzed with the Prism8 (GraphPad, San Diego, CA) statistical package. Results were expressed as mean ± standard error of the mean (SEM) and p values were determined using one-way ANOVA with Tukey's multiple comparison's test, or unpaired T-test when applicable. $p < 0.05$ was considered significant.

Acknowledgments: Teratomas were prepared, sectioned, and stained by UCLA Translational Pathology Core Laboratory.

Funding: These studies were funded by grants R21NS091654 and R01NS100979 (both to GSL) from the United States NIH/National Institute of Neurological Disorders and Stroke (NINDS), NIH NIAMS (R01 AR064327) (ADP), and the Philip Whitcome Pre-Doctoral Fellowship from the University of California, Los Angeles Molecular Biology Institute (MN). Work on urea cycle disorders is supported by the Swiss National Science Foundation (grant 320030_176088 to JH). No other authors have funding.

REFERENCES

1. Nettesheim S, Kölker S, Karall D, Häberle J, Posset R, Hoffmann GF, et al.; Arbeitsgemeinschaft für Pädiatrische Stoffwechselstörungen (APS); European registry and network for Intoxication type Metabolic Diseases (E-IMD); Erhebungseinheit für Seltene Pädiatrische Erkrankungen in Deutschland (ESPED); Austrian Metabolic Group; Swiss Paediatric Surveillance Unit (SPSU). Incidence, disease onset and short-term outcome in urea cycle disorders -cross-border surveillance in Germany, Austria and Switzerland [Internet]. Orphanet J Rare Dis. 2017 Jun;12(1):111. [cited 2017 Aug 30].
2. Summar ML, Koelker S, Freedenberg D, Le Mons C, Häberle J, Lee HS, et al.; European Registry and Network for Intoxication Type Metabolic Diseases (E-IMD). Electronic address: http://www.e-imd.org/en/index.phtml; Members of the Urea Cycle Disorders Consortium (UCDC). Electronic address: http://rarediseasesnetwork.epi.usf.edu/ucdc/. The incidence of urea cycle disorders. Mol Genet Metab. 2013 Sep-Oct;110(1-2):179–80.
3. Matsumoto S, Häberle J, Kido J, Mitsubuchi H, Endo F, Nakamura K. Urea cycle disorders-update. J Hum Genet. 2019 Sep;64(9):833–47.
4. Batshaw ML, Brusilow S, Waber L, Blom W, Brubakk AM, Burton BK, et al. Treatment of inborn errors of urea synthesis: activation of alternative pathways of waste nitrogen synthesis and excretion. N Engl J Med. 1982 Jun;306(23):1387–92.
5. Brusilow S, Tinker J, Batshaw ML. Amino acid acylation: a mechanism of nitrogen excretion in inborn errors of urea synthesis. Science. 1980 Feb;207(4431):659–61.
6. Hediger N, Landolt MA, Díez-Fernández C, Huemer M, Häberle J. The impact of ammonia levels and dialysis on outcome in 202 patients with neonatal onset urea cycle disorders. J Inherit Metab Dis. 2018 Jul;41(4):689–98.
7. Baruteau J, Perocheau DP, Hanley J, Lorvellec M, Rocha-Ferreira E, Karda R, et al. Argininosuccinic aciduria fosters neuronal nitrosative stress reversed by Asl gene transfer. Nat Commun. 2018 Aug;9(1):3505.
8. Lee EK, Hu C, Bhargava R, Rozengurt N, Stout D, Grody WW, et al. Long-term survival of the juvenile lethal arginase-deficient mouse with AAV gene therapy. Mol Ther. 2012 Oct;20(10):1844–51.
9. Wang L, Morizono H, Lin J, Bell P, Jones D, McMenamin D, et al. Preclinical evaluation of a clinical candidate AAV8 vector for ornithine transcarbamylase (OTC) deficiency reveals functional enzyme from each persisting vector genome. Mol Genet Metab. 2012 Feb;105(2):203–11.
10. Ye X, Whiteman B, Jerebtsova M, Batshaw ML. Correction of argininosuccinate synthetase (AS) deficiency in a murine model of citrullinemia with recombinant adenovirus carrying human AS cDNA. Gene Ther. 2000 Oct;7(20):1777–82.
11. Kok CY, Cunningham SC, Kuchel PW, Alexander IE. Insights into Gene Therapy for Urea Cycle Defects by Mathematical Modeling. Hum Gene Ther. 2019 Nov;30(11):1385–94.
12. Khoja S, Nitzahn M, Hermann K, Truong B, Borzone R, Willis B, et al. Conditional disruption of hepatic carbamoyl phosphate synthetase 1 in mice results in hyperammonemia without orotic aciduria and can be corrected by liver-directed gene therapy. Mol Genet Metab. 2018 Aug;124(4):243–53.
13. Nitzahn M, Allegri G, Khoja S, Truong B, Makris G, Häberle J, et al. Split AAV-Mediated Gene Therapy Restores Ureagenesis in a Murine Model of Carbamoyl Phosphate Synthetase 1 Deficiency. Mol Ther. 2020 Jul;28(7):1717–30.
14. Raper SE, Chirmule N, Lee FS, Wivel NA, Bagg A, Gao GP, et al. Fatal systemic inflammatory response syndrome in a ornithine transcarbamylase deficient patient following adenoviral gene transfer. Mol Genet Metab. 2003 Sep-Oct;80(1-2):148–58.
15. Tuchman M. Persistent acitrullinemia after liver transplantation for carbamylphosphate synthetase deficiency. N Engl J Med. 1989 Jun;320(22):1498–9.
16. Muraca M, Gerunda G, Neri D, Vilei MT, Granato A, Feltracco P, et al. Hepatocyte transplantation as a treatment for glycogen storage disease type 1a. Lancet. 2002 Jan;359(9303):317–8.
17. Stéphenne X, Debray FG, Smets F, Jazouli N, Sana G, Tondreau T, et al. Hepatocyte transplantation using the domino concept in a child with tetrabiopterin nonresponsive phenylketonuria. Cell Transplant. 2012;21(12):2765–70.
18. Stéphenne X, Najimi M, Sibille C, Nassogne MC, Smets F, Sokal EM. Sustained engraftment and tissue enzyme activity after liver cell transplantation for argininosuccinate lyase deficiency. Gastroenterology. 2006 Apr;130(4):1317–23.
19. Meyburg J, Hoffmann GF. Liver, liver cell and stem cell transplantation for the treatment of urea cycle defects. Mol Genet Metab. 2010;100 Suppl 1:S77–83.
20. Angarita SA, Truong B, Khoja S, Nitzahn M, Rajbhandari AK, Zhuravka I, et al. Human hepatocyte transplantation corrects the inherited metabolic liver disorder arginase deficiency in mice. Mol Genet Metab. 2018 Jun;124(2):114–23.
21. Takayama K, Akita N, Mimura N, Akahira R, Taniguchi Y, Ikeda M, et al. Generation of safe and therapeutically effective human induced pluripotent stem cell-derived hepatocyte-like cells for regenerative medicine. Hepatol Commun. 2017 Oct;1(10):1058–69.
22. Cong L, Ran FA, Cox D, Lin S, Barretto R, Habib N, et al. Multiplex genome engineering using CRISPR/Cas

systems. Science. 2013 Feb;339(6121):819–23.
23. Jinek M, Chylinski K, Fonfara I, Hauer M, Doudna JA, Charpentier E. A programmable dual-RNA-guided DNA endonuclease in adaptive bacterial immunity. Science. 2012 Aug;337(6096):816–21.
24. Martin RM, Ikeda K, Cromer MK, Uchida N, Nishimura T, Romano R, et al. Highly Efficient and Marker-free Genome Editing of Human Pluripotent Stem Cells by CRISPR-Cas9 RNP and AAV6 Donor-Mediated Homologous Recombination. Cell Stem Cell. 2019 May;24(5):821–828.e5.
25. Oceguera-Yanez F, Kim SI, Matsumoto T, Tan GW, Xiang L, Hatani T, et al. Engineering the AAVS1 locus for consistent and scalable transgene expression in human iPSCs and their differentiated derivatives. Methods. 2016 May;101:43–55.
26. Lee PC, Truong B, Vega-Crespo A, Gilmore WB, Hermann K, Angarita SA, et al. Restoring Ureagenesis in Hepatocytes by CRISPR/Cas9-mediated Genomic Addition to Arginase-deficient Induced Pluripotent Stem Cells. Mol Ther Nucleic Acids. 2016 Nov;5(11):e394.
27. Truong B. Human Induced Pluripotent Stem Cell- and mRNA-based Gene Therapy Strategies for Treatment of Arginase Deficiency [Internet]. UCLA; 2019 [cited 2021 Apr 26]. Available from: https://escholarship.org/uc/item/9gd7r3d8#main
28. Carpentier A, Nimgaonkar I, Chu V, Xia Y, Hu Z, Liang TJ. Hepatic differentiation of human pluripotent stem cells in miniaturized format suitable for high-throughput screen. Stem Cell Res (Amst). 2016 May;16(3):640–50.
29. Greenberg MV, Bourc'his D. The diverse roles of DNA methylation in mammalian development and disease. Nat Rev Mol Cell Biol. 2019 Oct;20(10):590–607.
30. Reizel Y, Sabag O, Skversky Y, Spiro A, Steinberg B, Bernstein D, et al. Postnatal DNA demethylation and its role in tissue maturation. Nat Commun. 2018 May;9(1):2040.
31. Xu CS, Chang CF. Expression profiles of the genes associated with metabolism and transport of amino acids and their derivatives in rat liver regeneration. Amino Acids. 2008 Jan;34(1):91–102.
32. Klatt D, Cheng E, Hoffmann D, Santilli G, Thrasher AJ, Brendel C, et al. Differential Transgene Silencing of Myeloid-Specific Promoters in the AAVS1 Safe Harbor Locus of Induced Pluripotent Stem Cell-Derived Myeloid Cells. Hum Gene Ther. 2020 Feb;31(3-4):199–210.
33. Lombardo A, Cesana D, Genovese P, Di Stefano B, Provasi E, Colombo DF, et al. Site-specific integration and tailoring of cassette design for sustainable gene transfer. Nat Methods. 2011 Aug;8(10):861–9.
34. Ordovás L, Boon R, Pistoni M, Chen Y, Wolfs E, Guo W, et al. Efficient Recombinase-Mediated Cassette Exchange in hPSCs to Study the Hepatocyte Lineage Reveals AAVS1 Locus-Mediated Transgene Inhibition. Stem Cell Reports. 2015 Nov;5(5):918–31.
35. Wang Y, Liang P, Lan F, Wu H, Lisowski L, Gu M, et al. Genome editing of isogenic human induced pluripotent stem cells recapitulates long QT phenotype for drug testing. J Am Coll Cardiol. 2014 Aug;64(5):451–9.
36. Zhang F, Frost AR, Blundell MP, Bales O, Antoniou MN, Thrasher AJ. A ubiquitous chromatin opening element (UCOE) confers resistance to DNA methylation-mediated silencing of lentiviral vectors. Mol Ther. 2010 Sep;18(9):1640–9.
37. Howell PM Jr, Liu Z, Khong HT. Demethylating Agents in the Treatment of Cancer. Pharmaceuticals (Basel). 2010 Jul;3(7):2022–44.
38. Spinelli JB, Yoon H, Ringel AE, Jeanfavre S, Clish CB, Haigis MC. Metabolic recycling of ammonia via glutamate dehydrogenase supports breast cancer biomass. Science. 2017 Nov;358(6365):941–6.
39. Finckh U, Kohlschütter A, Schäfer H, Sperhake K, Colombo JP, Gal A. Prenatal diagnosis of carbamoyl phosphate synthetase I deficiency by identification of a missense mutation in CPS1. Hum Mutat. 1998;12(3):206–11.
40. Häberle J, Koch HG. Genetic approach to prenatal diagnosis in urea cycle defects. Prenat Diagn. 2004 May;24(5):378–83.
41. Pettinato G, Lehoux S, Ramanathan R, Salem MM, He LX, Muse O, et al. Generation of fully functional hepatocyte-like organoids from human induced pluripotent stem cells mixed with Endothelial Cells. Sci Rep. 2019 Jun;9(1):8920.
42. Debnath T, Mallarpu CS, Chelluri LK. Development of Bioengineered Organ Using Biological Acellular Rat Liver Scaffold and Hepatocytes. Organogenesis. 2020 Apr;16(2):61–72.
43. Cascales-Campos PA, Ferreras D, Alconchel F, Febrero B, Royo-Villanova M, Martínez M, et al. Controlled donation after circulatory death up to 80 years for liver transplantation: pushing the limit again. Am J Transplant. 2020 Jan;20(1):204–12.
44. Ran FA, Hsu PD, Wright J, Agarwala V, Scott DA, Zhang F. Genome engineering using the CRISPR-Cas9 system. Nat Protoc. 2013 Nov;8(11):2281–308.
45. Yoshitoshi-Uebayashi EY, Toyoda T, Yasuda K, Kotaka M, Nomoto K, Okita K, et al. Modelling urea-cycle disorder citrullinemia type 1 with disease-specific iPSCs. Biochem Biophys Res Commun. 2017 May;486(3):613–9.
46. Pettinato G, Ramanathan R, Fisher RA, Mangino MJ, Zhang N, Wen X. Scalable Differentiation of Human iPSCs in a Multicellular Spheroid-based 3D Culture into Hepatocyte-like Cells through Direct Wnt/β-catenin Pathway Inhibition. Sci Rep. 2016 Sep;6(1):32888.
47. Holmgren G, Ulfenborg B, Asplund A, Toet K, Andersson CX, Hammarstedt A, et al. Characterization of Human Induced Pluripotent Stem Cell-Derived Hepatocytes with Mature Features and Potential for Modeling Metabolic Diseases. Int J Mol Sci. 2020 Jan;21(2):469.

Appendix A: Supplemental Table 1. Primers list

Primer Name	**Sequence (5'-3')**
qPCR	
GAPDH F	GCTCTCTGCTCCTCCTGTTC
GAPDH R	ACGACCAAATCCGTTGACTC
NAGS F	CAGTTCCAGACCTGCCATCACT
NAGS R	ATGTCCATGCGCTGCAAGAAGG
Endogenous CPS1 F	CAAGTTTTGCAGTGGAATCG
Endogenous CPS1 R	ACGGATCATCACTGGGTAGC
hcoCPS1 F	TACCCAACAACCTTGCTGTACCTC
hcoCPS1 R	GAGCTTGAGCGACTTTGAGTTCGT
OTC F	CCAGAGGCAGAAAACAGAAAG
OTC R	TTCTTGACAAGTAACACAACATCAAA
ASS1 F	CTTGGAGCTCTTCATGTACC
ASS1 R	GATACCTCGGGACTTCATTC
ASL F	TCGCTGTGCATGACCCATC
ASL R	CCAAACTGTCGGGGTTTTTCT
ARG1 F	TGGACAGACTAGGAATTGGCA
ARG1 R	CCAGTCCGTCAACATCAAAACT
CITRIN F	CACCAGGAAAGATGTTGAAGTG
CITRIN R	TCCATGGGTGTAACCTGACC
ORNT F	TTGCATCAGGGAGATCAAAA
ORNT R	GCAAGCCAGAGGCAAATC
AFP F	TGTACTGCAGAGATAAGTTTAGCTGAC
AFP R	TCCTTGTAAGTGGCTTCTTGAAC
CYP3A4 F	AAGTCGCCTCGAAGATACACA
CYP3A4 R	AAGGAGAGAACACTGCTCGTG
FAH F	ACCAGGATGTCTTCAATCAGC
FAH R	CAAGAACACTCTCGCCTCCT
GLUD1 F	CCATGGAGCTAGCAAAAAAGGG
GLUD1 R	TGATGGGTTTACCAGTAACACAG
GLS2 F1	CCAGCCAAGTCAGCTGTAT
GLS2 R1	AGACACCAACTTCTGGCAG
GLUL F	ATACGCTTGACTTTCTGTGGCTG
GLUL R	ATGGCCTGGACTTTCTCACC
Junction PCRs	
5' Junction F	GCTCAGGTCTGGTCTATCTGCCTGG
5' Junction R	CACCGTGGGCTTGTACTCGGTCA
3' Junction F	GCCGTGGATAGCGGTATCCC
3' Junction R	CCGAAGAGTGAGTTTGCCCAAGC
DNA Methylation	
EF1α Promoter F	TAAGGGGGAGGATTGGGAAG
EF1α Promoter R	AAAAATCACRTACTACAACCAAATA